

Anomalous quartic gauge couplings at a muon collider

Brad Abbott,¹ Aram Apyan,^{2,*} Bianca Azartash-Namin,¹ Veena Balakrishnan,¹ Jeffrey Berryhill,³ Shih-Chieh Hsu,⁴ Sergo Jindariani,³ Mayuri Kawale,¹ Elham Khoda,⁴ Ryan Parsons,¹ Alexander Schuy,⁴ Michael Strauss,¹ John Stupak,¹ and Connor Waits¹

¹*Homer L. Dodge Department of Physics and Astronomy,
University of Oklahoma, Norman OK, USA*

²*Department of Physics, Brandeis University, Waltham MA, USA*

³*Fermi National Accelerator Laboratory, Batavia IL, USA*

⁴*Department of Physics, University of Washington, Seattle WA, USA*

(Dated: March 16, 2022)

Abstract

Prospects for searches of anomalous quartic gauge couplings at a future high-energy muon collider using the production of WW boson pairs are reported. Muon-muon collision events are simulated at $\sqrt{s} = 6$ TeV corresponding to an integrated luminosity of 4 ab^{-1} . The simulated events are used to study the $WW\nu\nu$ and $WW\mu\mu$ final states with the W bosons decaying hadronically. The events are analyzed to report expected constraints on the structure of quartic vector boson interactions in the framework of dimension-8 effective field theory operators.

Submitted to the Proceedings of the US Community Study
on the Future of Particle Physics (Snowmass 2021)

* arapyan@brandeis.edu

I. INTRODUCTION

Vector boson scattering (VBS) processes probe the structure of the triple and quartic electroweak (EW) gauge boson self-interactions [1, 2]. Deviations of measurements with respect to the Standard Model (SM) predictions could indicate the presence of anomalous quartic gauge couplings (aQGCs) [3, 4]. Measurements of the VBS processes at the CERN LHC by the ATLAS and CMS Collaborations have reported constraints on aQGCs in the framework of dimension-8 effective field theory (EFT) operators [5–21]. The LHC results so far have been restricted to operators that introduce aQGCs without modifying the triple gauge couplings. In addition, the EFT is not a complete model and the presence of nonzero aQGCs will violate tree-level unitarity at sufficiently high energy [4]. A few of these LHC results address the unitarity issues in some form but not all of them. Prospects of aQGC searches using the scattering of W and Z bosons at high-energy electron-positron (e^+e^-) colliders were reported in Ref. [22].

The goal of this paper is to study the prospects of aQGC searches at a future multi-TeV muon collider via $W^\pm W^\mp$ production. A comprehensive physics case for a future high energy muon collider, with center of mass energies from 1 to 100 TeV, is reported in Ref. [23]. A muon collider has considerable advantages compared to proposed linear and circular electron-positron (e^+e^-) [24–27] and circular proton-proton machines [28, 29] in terms of having a high energy and high luminosity reach with a relatively clean environment. However, compared to e^+e^- colliders, the effects of backgrounds induced by the muon beam decays, referred as the beam induced background, are important and need to be studied in detail [30].

A multi-TeV muon collider is a “high-luminosity weak boson collider” [31] and provides a great opportunity to study VBS processes. Prospects of measuring the scattering of longitudinally polarized Z boson pairs at a muon collider were reported in Ref. [32]. This work focuses on the prospects of aQGC searches using events with oppositely-charged $W^\pm W^\mp$ boson pairs. The studies are performed in $WW\nu\nu$ and $WW\mu\mu$ channels, where the WW boson pairs are produced in association with two neutrinos and two muons, respectively. Figure 1 shows representative Feynman diagrams involving quartic vertices for the $WW\nu\nu$ (left) and $WW\mu\mu$ (right) channels.

A muon-muon ($\mu^+\mu^-$) collider at $\sqrt{s} = 6$ TeV with a data sample corresponding to an integrated luminosity of 4 ab^{-1} is considered for this study. Events are selected targeting

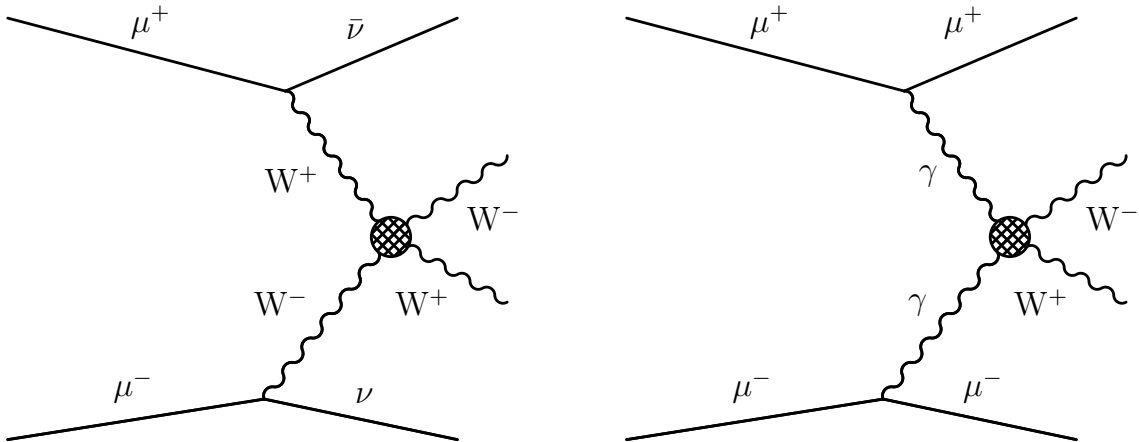


FIG. 1. Representative Feynman diagrams of the $WW\nu\nu$ (left) and $WW\mu\mu$ (right) processes. New physics (represented by a hatched circle) in the EW sector can modify the quartic gauge couplings.

hadronically decaying W bosons to target the final states with the highest branching ratios. Ten independent charge conjugate and parity conserving dimension-8 effective operators are considered [3]. The S0 and S1 operators are constructed from the covariant derivative of the Higgs doublet. The T0, T1, T2, T6, and T7 operators are constructed from the $SU_L(2)$ gauge fields. The mixed operators M0, M1, and M7 involve the $SU_L(2)$ gauge fields and the Higgs doublet. The $WW\nu\nu$ and $WW\mu\mu$ channels are analyzed separately.

II. EVENT SIMULATION

MADGRAPH5_aMC@NLO 3.1.1 [33, 34] and WHIZARD 3 [35, 36] Monte Carlo (MC) event generators are used to simulate the signal and background contributions. The aQGC processes are simulated using MADGRAPH5_aMC@NLO at leading order (LO). The contributions of the interference terms between the EFT operators and the SM amplitude are simulated separately from the contributions of the square of the amplitudes involving the EFT operators. The SM $WW\nu\nu$ and $WW\mu\mu$ background processes are simulated with MADGRAPH5_aMC@NLO. These SM processes are also simulated with WHIZARD at LO and good agreement is seen with MADGRAPH5_aMC@NLO predictions.

Other background processes contributing to the $WW\nu\nu$ are simulated following the corresponding studies for the e^+e^- collider in Ref. [22]. The $WZ\mu\nu$, $ZZ\mu\mu$, $WW\mu\mu$, and WWZ ,

with the Z boson decaying to neutrinos, processes are simulated using WHIZARD. The beam initial state radiation implemented in WHIZARD is included in the simulation.

The parton showering and hadronization are simulated using PYTHIA 8.306 [37]. Detector effects are simulated using DELPHES 3.5 [38] with a generic muon collider detector description. The beam induced background effects are not considered in this description. The reconstructed muons and electrons have an absolute pseudorapidity of less than 2.5. Jets are clustered from the reconstructed objects using FASTJET [39] with the VALENCIA algorithm [40]. Exclusive clustering is performed to reconstruct exactly two jets in the final state with distance parameters of 1.2 and 1.5 in the $WW\nu\nu$ and $WW\mu\mu$ channels, respectively. The reconstructed muons and electrons are not included as inputs to the clustering.

III. EVENT SELECTION

Events are selected targeting hadronically decaying WW boson pairs with a large invariant mass. Candidate WW boson pairs are selected by requiring two jets with $50 < m_W < 100$ GeV, where m_W is the mass of the jet. The two jets in the $WW\nu\nu$ channel are also required to have transverse momenta (p_T) greater than 100 GeV and $|\cos\theta| < 0.8$, where θ is the angle of the jet with respect to the beam axis.

The $WW\nu\nu$ channel is targeted by vetoing events with a reconstructed electron or muon with a momentum greater than 3 GeV. This requirement significantly reduces the $WW\mu\mu$ background contribution in this channel. The photon induced $WW\mu\mu$ background contribution can be reduced even further with a detector with higher forward rapidity coverage. The events are also required to have a missing mass (m_{miss}) greater than 200 GeV as the $WW\nu\nu$ channel contains two neutrinos in the final state. The m_{miss} is defined as

$$m_{\text{miss}} = \sqrt{(\sqrt{s} - E_{\text{WW}})^2 - |\vec{p}_{\text{WW}}|^2}, \quad (1)$$

where E_{WW} and \vec{p}_{WW} are the energy and momentum of the WW boson pairs, respectively. This requirement removes events where neutrinos are produced from Z boson decays and reduces the contributions of the s-channel WW and quantum chromodynamics two jet processes.

The $WW\mu\mu$ channel is targeted by requiring two oppositely charged muons with momenta greater than 3 GeV. The dominant background contribution is the SM production of $WW\mu\mu$

where the photon induced final state muons tend to be very forward. The mass of the dimuon pair is required to be greater than 106 GeV to reduce the contribution of events where the muons are produced from the Z boson decays.

IV. RESULTS

The selected events are used to constrain aQGCs in the EFT framework. The expected yields for the different SM processes and for an illustrative aQGC parameter in the $WW\nu\nu$ channel are given in Table I. The expected yield of the SM $WW\mu\mu$ contribution in the $WW\mu\mu$ channel is 10,703 while the expected yield of an illustrative aQGC parameter $f_{T,1}/\Lambda^4 = 1 \text{ TeV}^{-4}$ is 265,307.

TABLE I. The expected yields for various SM background processes in the $WW\nu\nu$ channel. The uncertainties due to the limited number of MC simulated events are negligible.

Process	Yields in $WW\nu\nu$ channel
$WW\nu\nu$	1,082,800
$WW\mu\mu$	11,181,200
$WZ\mu\nu$	1,132,800
$ZZ\mu\mu$	3,319
$WWZ (Z \rightarrow \nu\nu)$	14,396
Total background	12,331,715
$f_{T,1}/\Lambda^4 = 1 \text{ TeV}^{-4}$	20,337,080

Statistical analysis of the event yields is performed separately in the $WW\nu\nu$ and $WW\mu\mu$ channels with a fit to the invariant mass distribution of the WW pair (m_{WW}). The distributions of m_{WW} after the event selection are shown in Fig. 2 for the $WW\nu\nu$ (left) and $WW\mu\mu$ (right) channels, respectively. The expected 95% confidence level (CL) lower and upper limits on the aQGC parameters f/Λ^4 , where f is the Wilson coefficient of the given operator and Λ is the energy scale of new physics, are derived from Wilk's theorem [41] assuming that the profile likelihood test statistic is χ^2 distributed [42]. No nuisance parameters corresponding to systematic uncertainties are included in the fits.

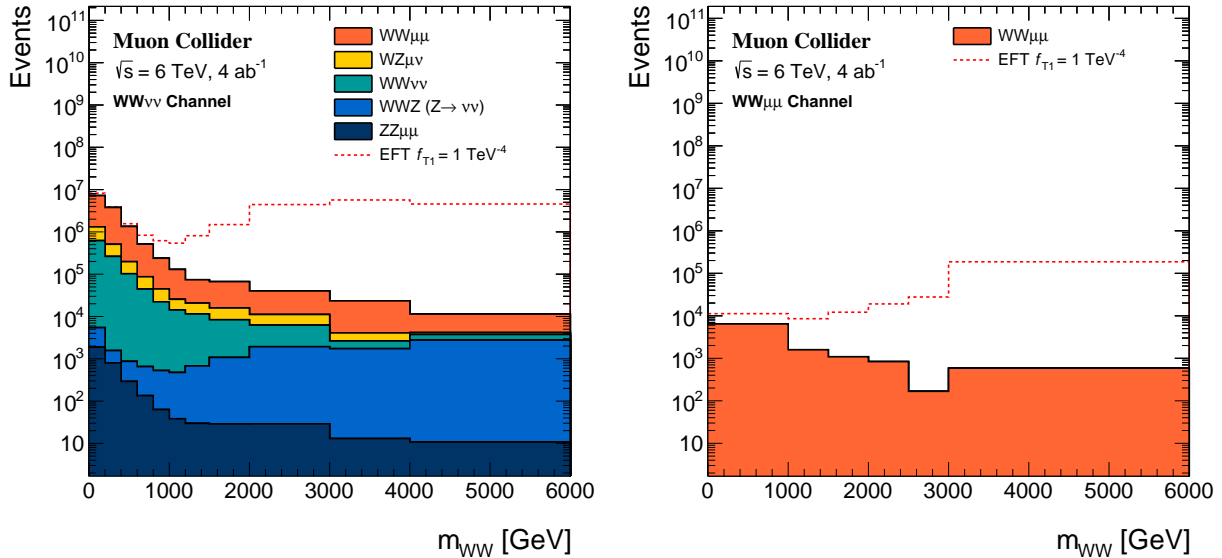


FIG. 2. Distributions of m_{WW} in the $WW\nu\nu$ (left) and $WW\mu\mu$ (right) channels, respectively, after the event selection. The dashed lines show the signal predictions for one illustrative aQGC parameter. The overflow is included in the last bin.

Table II shows the individual lower and upper limits obtained by setting all other aQGCs parameters to zero in the $WW\nu\nu$ channel for the S0, S1, M0, M1, M7, T0, T1, and T2 operators. The $WW\mu\mu$ contribution in the $WW\nu\nu$ channel is treated as a background process and is taken from the SM in the statistical analysis.

Table III shows the individual lower and upper limits obtained by setting all other aQGCs parameters to zero in the $WW\mu\mu$ channel for the T0, T1, T2, T6, and T7 operators. The operators T6 and T7 are especially interesting for the $WW\mu\mu$ channel as the presence of these operators does not modify the SM quartic $WWWW$ vertex.

These new results give stringent constraints on the aQGC parameters for the S0, S1, M0, M1, M6, M7, T0, T1, T2, T5, and T6 operators. It has to be noted that the given limits do not include procedures to avoid tree-level unitarity violation. The effects of the beam induced backgrounds are also not included. These considerations are deferred to future work.

TABLE II. Expected lower and upper 95% CL limits on the parameters of the quartic operators S0, S1, M0, M1, M7, T0, T1, and T2 in the $WW\nu\nu$ channel.

$WW\nu\nu$	Limits (TeV^{-4})
$f_{M,0}/\Lambda^4$	$[-0.032, 0.035]$
$f_{M,1}/\Lambda^4$	$[-0.088, 0.065]$
$f_{M,7}/\Lambda^4$	$[-0.12, 0.17]$
$f_{S,0}/\Lambda^4$	$[-0.22, 0.20]$
$f_{S,1}/\Lambda^4$	$[-0.14, 0.14]$
$f_{T,0}/\Lambda^4$	$[-0.0062, 0.0030]$
$f_{T,1}/\Lambda^4$	$[-0.0082, 0.0031]$
$f_{T,2}/\Lambda^4$	$[-0.0096, 0.0046]$

TABLE III. Expected lower and upper 95% CL limits on the parameters of the quartic operators T0, T1, T2, T6, and T7 in the $WW\mu\mu$ channel.

$WW\mu\mu$	Limits (TeV^{-4})
$f_{T,0}/\Lambda^4$	$[-0.04, 0.028]$
$f_{T,1}/\Lambda^4$	$[-0.025, 0.0095]$
$f_{T,2}/\Lambda^4$	$[-0.12, 0.068]$
$f_{T,6}/\Lambda^4$	$[-0.034, 0.033]$
$f_{T,7}/\Lambda^4$	$[-0.043, 0.038]$

V. SUMMARY

Prospects for searches of anomalous quartic gauge couplings at a future high-energy muon collider using the production of WW boson pairs are studied. Muon-muon collision events are simulated at $\sqrt{s} = 6$ TeV corresponding to an integrated luminosity of 4 ab^{-1} . The simulated events are used to study $WW\nu\nu$ and $WW\mu\mu$ final states with the W bosons decaying hadronically. Contributions of the SM background processes are considered in the analysis. Constraints on the quartic vector boson interactions in the framework of dimension-8 effective field theory operators are obtained with stringent limits set on the effective field

theory operators S0, S1, M0, M1, M7, T0, T1, T2, T6, and T7.

- [1] B. W. Lee, C. Quigg, and H. B. Thacker, The strength of weak interactions at very high-energies and the Higgs boson mass, *Phys. Rev. Lett.* **38**, 883 (1977).
- [2] B. W. Lee, C. Quigg, and H. B. Thacker, Weak interactions at very high-energies: the role of the Higgs boson mass, *Phys. Rev. D* **16**, 1519 (1977).
- [3] O. J. P. Éboli, M. C. Gonzalez-Garcia, and J. K. Mizukoshi, $pp \rightarrow jje^\pm \mu^\pm \nu\nu$ and $jje^\pm \mu^\mp \nu\nu$ at $\mathcal{O}(\alpha_{\text{em}}^6)$ and $\mathcal{O}(\alpha_{\text{em}}^4 \alpha_s^2)$ for the study of the quartic electroweak gauge boson vertex at CERN LHC, *Phys. Rev. D* **74**, 073005 (2006), arXiv:hep-ph/0606118 [hep-ph].
- [4] E. d. S. Almeida, O. J. P. Éboli, and M. C. Gonzalez-Garcia, Unitarity constraints on anomalous quartic couplings, *Phys. Rev. D* **101**, 113003 (2020), arXiv:2004.05174 [hep-ph].
- [5] G. Aad *et al.* (ATLAS), Evidence for electroweak production of $W^\pm W^\pm jj$ in pp collisions at $\sqrt{s} = 8$ TeV with the ATLAS detector, *Phys. Rev. Lett.* **113**, 141803 (2014), arXiv:1405.6241 [hep-ex].
- [6] V. Khachatryan *et al.* (CMS), Study of vector boson scattering and search for new physics in events with two same-sign leptons and two jets, *Phys. Rev. Lett.* **114**, 051801 (2015), arXiv:1410.6315 [hep-ex].
- [7] A. M. Sirunyan *et al.* (CMS), Observation of electroweak production of same-sign W boson pairs in the two jet and two same-sign lepton final state in proton-proton collisions at $\sqrt{s} = 13$ TeV, *Phys. Rev. Lett.* **120**, 081801 (2018), arXiv:1709.05822 [hep-ex].
- [8] M. Aaboud *et al.* (ATLAS), Measurement of $W^\pm W^\pm$ vector boson scattering and limits on anomalous quartic gauge couplings with the ATLAS detector, *Phys. Rev. D* **96**, 012007 (2017), arXiv:1611.02428 [hep-ex].
- [9] G. Aad *et al.* (ATLAS), Measurements of $W^\pm Z$ production cross sections in pp collisions at $\sqrt{s} = 8$ TeV with the ATLAS detector and limits on anomalous gauge boson self-couplings, *Phys. Rev. D* **93**, 092004 (2016), arXiv:1603.02151 [hep-ex].
- [10] A. M. Sirunyan *et al.* (CMS), Measurement of electroweak WZ boson production and search for new physics in WZ + two jets events in pp collisions at $\sqrt{s} = 13$ TeV, *Phys. Lett. B* **795**, 281 (2019), arXiv:1901.04060 [hep-ex].

- [11] A. M. Sirunyan *et al.* (CMS), Measurement of vector boson scattering and constraints on anomalous quartic couplings from events with four leptons and two jets in proton-proton collisions at $\sqrt{s} = 13$ TeV, *Phys. Lett. B* **774**, 682 (2017), arXiv:1708.02812 [hep-ex].
- [12] V. Khachatryan *et al.* (CMS), Evidence for exclusive $\gamma\gamma \rightarrow W^+W^-$ production and constraints on anomalous quartic gauge couplings in pp collisions at $\sqrt{s} = 7$ and 8 TeV, *JHEP* **08**, 119, arXiv:1604.04464 [hep-ex].
- [13] V. Khachatryan *et al.* (CMS), Measurement of the cross section for electroweak production of $Z\gamma$ in association with two jets and constraints on anomalous quartic gauge couplings in proton-proton collisions at $\sqrt{s} = 8$ TeV, *Phys. Lett. B* **770**, 380 (2017), arXiv:1702.03025 [hep-ex].
- [14] V. Khachatryan *et al.* (CMS), Measurement of electroweak-induced production of $W\gamma$ with two jets in pp collisions at $\sqrt{s} = 8$ TeV and constraints on anomalous quartic gauge couplings, *JHEP* **06**, 106, arXiv:1612.09256 [hep-ex].
- [15] M. Aaboud *et al.* (ATLAS), Studies of $Z\gamma$ production in association with a high-mass dijet system in pp collisions at $\sqrt{s} = 8$ TeV with the ATLAS detector, *JHEP* **07**, 107, arXiv:1705.01966 [hep-ex].
- [16] M. Aaboud *et al.* (ATLAS), Search for anomalous electroweak production of WW/WZ in association with a high-mass dijet system in pp collisions at $\sqrt{s} = 8$ TeV with the ATLAS detector, *Phys. Rev. D* **95**, 032001 (2017), arXiv:1609.05122 [hep-ex].
- [17] A. M. Sirunyan *et al.* (CMS), Search for anomalous electroweak production of vector boson pairs in association with two jets in proton-proton collisions at 13 TeV, *Phys. Lett. B* **798**, 134985 (2019), arXiv:1905.07445 [hep-ex].
- [18] A. M. Sirunyan *et al.* (CMS), Measurements of production cross sections of WZ and same-sign WW boson pairs in association with two jets in proton-proton collisions at $\sqrt{s} = 13$ TeV, *Phys. Lett. B* **809**, 135710 (2020), arXiv:2005.01173 [hep-ex].
- [19] A. M. Sirunyan *et al.* (CMS), Evidence for electroweak production of four charged leptons and two jets in proton-proton collisions at $\sqrt{s} = 13$ TeV, *Phys. Lett. B* **812**, 135992 (2021), arXiv:2008.07013 [hep-ex].
- [20] A. M. Sirunyan *et al.* (CMS), Observation of electroweak production of $W\gamma$ with two jets in proton-proton collisions at $\sqrt{s} = 13$ TeV, *Phys. Lett. B* **811**, 135988 (2020), arXiv:2008.10521 [hep-ex].

- [21] A. Tumasyan *et al.* (CMS), Measurement of the electroweak production of $Z\gamma$ and two jets in proton-proton collisions at $\sqrt{s} = 13$ TeV and constraints on anomalous quartic gauge couplings, *Phys. Rev. D* **104**, 072001 (2021), arXiv:2106.11082 [hep-ex].
- [22] C. Fleper, W. Kilian, J. Reuter, and M. Sekulla, Scattering of W and Z Bosons at High-Energy Lepton Colliders, *Eur. Phys. J. C* **77**, 120 (2017), arXiv:1607.03030 [hep-ph].
- [23] H. Al Ali *et al.*, The Muon Smasher’s Guide, arXiv:2103.14043 [hep-ph] (2021).
- [24] P. Bambade *et al.*, The International Linear Collider: A Global Project, arXiv:1903.01629 [hep-ex] (2019).
- [25] T. K. Charles *et al.* (CLICdp, CLIC), The Compact Linear Collider (CLIC) - 2018 Summary Report (2018) arXiv:1812.06018 [physics.acc-ph].
- [26] A. Abada *et al.* (FCC), FCC-ee: The Lepton Collider: Future Circular Collider Conceptual Design Report Volume 2, *Eur. Phys. J. ST* **228**, 261 (2019).
- [27] M. Dong *et al.* (CEPC Study Group), CEPC Conceptual Design Report: Volume 2 - Physics & Detector (2018) arXiv:1811.10545 [hep-ex].
- [28] A. Abada *et al.* (FCC), FCC-hh: The Hadron Collider: Future Circular Collider Conceptual Design Report Volume 3, *Eur. Phys. J. ST* **228**, 755 (2019).
- [29] CEPC Conceptual Design Report: Volume 1 - Accelerator (2018) arXiv:1809.00285 [physics.acc-ph].
- [30] N. Bartosik *et al.*, Detector and Physics Performance at a Muon Collider, *JINST* **15**, P05001, arXiv:2001.04431 [hep-ex].
- [31] A. Costantini, F. De Lillo, F. Maltoni, L. Mantani, O. Mattelaer, R. Ruiz, and X. Zhao, Vector boson fusion at multi-TeV muon colliders, *JHEP* **09**, 080, arXiv:2005.10289 [hep-ph].
- [32] T. Yang, S. Qian, Z. Guan, C. Li, F. Meng, J. Xiao, M. Lu, and Q. Li, Longitudinally polarized ZZ scattering at a muon collider, *Phys. Rev. D* **104**, 093003 (2021), arXiv:2107.13581 [hep-ph].
- [33] R. Frederix and S. Frixione, Merging meets matching in MC@NLO, *JHEP* **12**, 061, arXiv:1209.6215 [hep-ph].
- [34] J. Alwall, R. Frederix, S. Frixione, V. Hirschi, F. Maltoni, O. Mattelaer, H. S. Shao, T. Stelzer, P. Torrielli, and M. Zaro, The automated computation of tree-level and next-to-leading order differential cross sections, and their matching to parton shower simulations, *JHEP* **07**, 079, arXiv:1405.0301 [hep-ph].

- [35] M. Moretti, T. Ohl, and J. Reuter, O'Mega: An Optimizing matrix element generator (2001) p. 1981, arXiv:hep-ph/0102195.
- [36] W. Kilian, T. Ohl, and J. Reuter, WHIZARD: Simulating Multi-Particle Processes at LHC and ILC, *Eur. Phys. J. C* **71**, 1742 (2011), arXiv:0708.4233 [hep-ph].
- [37] T. Sjöstrand, S. Ask, J. R. Christiansen, R. Corke, N. Desai, P. Ilten, S. Mrenna, S. Prestel, C. O. Rasmussen, and P. Z. Skands, An Introduction to PYTHIA 8.2, *Comput. Phys. Commun.* **191**, 159 (2015), arXiv:1410.3012 [hep-ph].
- [38] J. de Favereau, C. Delaere, P. Demin, A. Giammanco, V. Lemaître, A. Mertens, and M. Selvaggi (DELPHES 3), DELPHES 3, A modular framework for fast simulation of a generic collider experiment, *JHEP* **02**, 057, arXiv:1307.6346 [hep-ex].
- [39] M. Cacciari, G. P. Salam, and G. Soyez, FastJet user manual, *Eur. Phys. J. C* **72**, 1896 (2012), arXiv:1111.6097 [hep-ph].
- [40] M. Boronat, J. Fuster, I. Garcia, E. Ros, and M. Vos, A robust jet reconstruction algorithm for high-energy lepton colliders, *Phys. Lett. B* **750**, 95 (2015), arXiv:1404.4294 [hep-ex].
- [41] S. S. Wilks, The Large-Sample Distribution of the Likelihood Ratio for Testing Composite Hypotheses, *The Annals of Mathematical Statistics* **9**, 60 (1938).
- [42] G. Cowan, K. Cranmer, E. Gross, and O. Vitells, Asymptotic formulae for likelihood-based tests of new physics, *Eur. Phys. J. C* **71**, 1554 (2011), [Erratum: DOI:10.1140/epjc/s10052-013-2501-z], arXiv:1007.1727 [physics.data-an].